POROELASTICITY 1D CODE

NAREN VOHRA, MALGORZATA PESZYNSKA

GitHub Link : https://github.com/nvohra0016/Biot1D-MATLAB

1. Introduction

In this document we provide the details of a one dimensional (1D) implementation of Biot's poroelasticity system [3] in MATLAB. We use a 3 field, mixed finite element scheme [7] in which the displacement is approximated in the space of piecewise linear polynomials, pressure in the space of piecewise constants, and fluxes in the lowest order Raviart-Thomas space.

1.1. Credits and Use.

This code is part of the MPower toolbox:
`http://sites.science.oregonstate.edu/~mpesz/mpower/`
The code is publicly available through GitHub: https://github.com/nvohra0016/Biot1D-MATLAB. The implementation is licensed under the Creative Commons CC BY-NC-ND 4.0 Attribution-NonCommercial-NoDerivatives 4.0 International license and the GNU GPL license. To view the full license, please see the file License.md in the GitHub repository. To view the funding sources, please see the Acknowledgement section (Section 7.1) in this document. For any questions, please feel free to contact the authors via email:

Naren Vohra: `vohran@oregonstate.edu`
Website: https://nvohra0016.github.io
Malgorzata Peszynska: `malgo.peszynska@oregonstate.edu`
Website: https://sites.science.oregonstate.edu/ mpesz/index.html

2. Governing Equations

Let $\Omega = (a, b) \subset \mathbb{R}$ represent a porous medium that is fully saturated with a fluid. For any $x \in \Omega,\ t > 0$, let $u(x, t)$ denote the displacement of the medium and $p(x, t)$ denote the pressure. Then, $\forall x \in \Omega,\ t > 0$ as in [5](Pg. 114)

$$-\frac{\partial}{\partial x}\left[(\lambda + 2\mu)\frac{\partial u}{\partial x}\right] + \alpha\frac{\partial p}{\partial x} = f + \overline{\rho}G\frac{\partial D}{\partial x}, \tag{1a}$$

$$\frac{\partial \eta_f}{\partial t} + \frac{\partial q_f}{\partial x} = \frac{g}{\rho_f}, \tag{1b}$$

$$q_f = -\frac{\kappa}{\mu_f}\left[\frac{\partial p}{\partial x} - \rho_f G\frac{\partial D}{\partial x}\right], \tag{1c}$$

where η_f denotes the total fluid content, given by

$$\eta_f(x, t) = \beta_f \phi p + \alpha\frac{\partial u}{\partial x},\ \forall x \in \Omega, t > 0, \tag{2}$$

Last updated: 4 December 2022.

Variable	Description/ SI Unit	Preferred units
u	Displacement [m]	
p	Pressure [Pa]	[MPa]
q_f	Flux [m/s]	[m/hr]
η_f	Total fluid content [−]	
D	Depth [m]	[m]
f	Volumetric body force [N/m^3]	
g	Mass source rate [kg/m^3 s]	
Parameter		Typical value
E	Young's modulus [Pa]	Sand (medium/fine): $12-20$[MPa] [4](Pg. 407) Silt: $2-20$[MPa] [4](Pg. 407) Clay (medium/firm): $15-50$[MPa] [4](Pg. 406)
ν	Poisson's ratio [−]	Sand (medium/ fine): 0.25 [4](Pg. 407) Silt : $0.30-0.35$ [4](Pg. 407) Clay(medium/firm): 0.30 [4](Pg. 406)
λ μ	Lamé parameter [Pa]; $\frac{E\nu}{(1+\nu)(1-2\nu)}$ Lamé parameter [Pa]; $\frac{E}{2(1+\nu)}$	
ρ_f	Fluid density [kg/m^3]	998.21[kg/m^3] (at 20° C) [6]
ρ_s	Solid particles density [kg/m^3]	Sand: 2650[kg/m^3] [1](Pg. 22) Clay: 2700[kg/m^3] [1](Pg. 22)
ϕ	Porosity [−]	Sand(medium/fine): $0.30-0.35$ [2](Pg. 74) Silt: $0.4-0.5$ [2](Pg. 74) Clay: $0.45-0.55$ [2](Pg. 74)
$\overline{\rho}$	Average density of media [kg/m^3]; $\rho_f\phi+\rho_s(1-\phi)$	$-$[kg/m^3]
β_f	Fluid compressibility [1/Pa]; $\frac{1}{\rho_f}\frac{\partial\rho_f}{\partial p}$	4.16×10^{-4}[1/MPa] [6]
κ	Permeability [m^2]	Sand: $10^{-13}-10^{-11}$[m^2] (saturated) [4](Pg. 373) Silt: $10^{-15}-10^{-13}$[m^2] (saturated) [4](Pg. 373) Clay: $10^{-18}-10^{-15}$[m^2] (saturated) [4](Pg. 373)
μ_f	Fluid viscosity [Pa s]	2.7822×10^{-13}[MPa hr] (at 20°C) [6]
G	Acceleration due to gravity [m/s^2]	1.27290528×10^{8}[m/hr^2] (at Anchorage, Alaska) [6]

TABLE 1. Variables and parameters used throughout the article.

q_f is the flux, and D is the depth. The other variables and physical parameters used in (1) are described in Table 1. Mechanical gravitational effects are in included in (1a) using the term $\overline{\rho}G\frac{\partial D}{\partial x}$ and the hydrological gravitational effects are included in Darcy's law (1c) using $\rho_f G\frac{\partial D}{\partial x}$. Here, the depth D is a linear function which depends on the physical scenario. For example, if $\Omega=(a,b)$ represents a vertical column of soil with $x=a$ being the top and $x=b$ being the bottom, then

$$D(x)=x-a,\ \forall x\in\Omega. \tag{3}$$

If $x=a$ is the bottom then

$$D(x)=b-x,\ \forall x\in\Omega. \tag{4}$$

For a horizontal domain we have $D=0$.

2.1. **Boundary and initial conditions.** The two distinct sets of boundary conditions correspond to mechanical deformation [M] and hydrological flow [H]. Mixed boundary conditions

corresponding to [M] are

$$u = u_D, \text{ on } \Gamma_{MD}, \tag{5a}$$
$$\tilde{\sigma} n = \sigma_N, \text{ on } \Gamma_{MN}, \tag{5b}$$

where $\Gamma_{MD}, \Gamma_{MN} \subset \{a, b\}$, $\Gamma_{MD} \cup \Gamma_{MN} = \{a, b\}$, and $\Gamma_{MD} \neq \emptyset$, and n is the outward unit normal to Γ_{MN}. The boundary conditions corresponding to [H] are

$$p = p_D, \text{ on } \Gamma_{HD}, \tag{6a}$$
$$q_f n = q_N, \text{ on } \Gamma_{HN}, \tag{6b}$$

where $\Gamma_{HD}, \Gamma_{HN} \subset \{a, b\}$.

The initial condition is given on the fluid content η_f as

$$\eta_f(x, 0) = \eta_{f_{init}}(x) \ \forall x \in (a, b), \tag{7}$$

although in practise it is sometimes computed using initial conditions on p and $\frac{\partial u}{\partial x}$.

We test multiple examples with different combinations of the Dirichlet (D) and Neumann (N) boundary conditions. In our notation, we specify the deformation boundary conditions followed by the flow boundary conditions: [MMHH]. An example of our notation is as follows: a case with Dirichlet boundary conditions for [M] and mixed boundary conditions for [H], with $\Gamma_{HD} = \{a\}$ and $\Gamma_{HN} = \{b\}$ is denoted as [DDDN].

3. Discretization

Consider the discretization of $\Omega = (a, b)$ into M cells using a grid $\mathscr{T}_h = (\omega_j)_j$ so that $\Omega = \cup_{j=1}^{M} \omega_j$, where the cell $\omega_j = [x_{j-\frac{1}{2}}, x_{j+\frac{1}{2}}]$ has center x_j, $1 \leq j \leq M$ and size $|\omega_j| = x_{j+\frac{1}{2}} - x_{j-\frac{1}{2}} = h_j$. Consider a uniform time step $\tau > 0$ so that the n^{th} time step is given by $t_n = n\tau$.

3.1. Approximation spaces.

Here we describe the finite dimensional function spaces built on $\mathscr{T}_h$ in which we seek an approximate solution to (1). Let

$$V_h = \{\phi_h \in C^0(\Omega) \mid \phi_h|_{\omega_j} = a_j x + b_j, \ a_j, b_j \in \mathbb{R}, \ 1 \leq j \leq M\}, \tag{8a}$$

be the space of continuous, piecewise linear functions on Ω and

$$V_{h,0} \subset V_h, \ V_{h,0} = \{\phi_h \in V_h \mid \phi_h|_{\Gamma_{MD}} = 0\}, \tag{8b}$$

be the subspace of V_h containing functions which vanish on Γ_{MD}. Let

$$M_h = \{\eta_h \mid \eta_h|_{\omega_j} = const, \ \forall \ 1 \leq j \leq M\}, \tag{8c}$$

be the space of piecewise constants on Ω and

$$X_h = \{\psi_h \in C^0(\Omega) \mid \psi_h|_{\omega_j} = a_j x + b_j, a_j, b_j \in \mathbb{R}, \ 1 \leq j \leq M\}, \tag{8d}$$

be the lowest order Raviart-Thomas space of functions with

$$X_{h,0} \subset X_h, \ X_{h,0} = \{\psi_h \in X_h \mid \psi_h|_{\Gamma_{HN}} = 0\}, \tag{9}$$

its subspace consisting of functions which vanish on Γ_{HN}. The basis functions of these spaces are described in Section 7.

3.2. **Discrete problem.** Let $\tilde{u_D}^n \in V_h$, be such that

$$\tilde{u_D}^n(x_{i-\frac{1}{2}}) = u_D(x_{i-\frac{1}{2}}, t_n),\ \forall x_{i-\frac{1}{2}} \in \Gamma_{MD},\ n \geq 1, \tag{10a}$$

and $\tilde{q_N}^n \in X_h$ be such that

$$\tilde{q_N}^n(x_{i-\frac{1}{2}}) = q_N(x_{i-\frac{1}{2}}, t_n),\ \forall x_{i-\frac{1}{2}} \in \Gamma_{HN},\ n \geq 1, \tag{10b}$$

whenever $|\Gamma_{HN}| > 0$. The three field discrete problem corresponding to (1) is given by: find $u_h^n \in \tilde{u_D}^n + V_{h,0},\ p_h^n \in M_h,\ q_{f_h}^n \in \tilde{q_N}^n + X_{h,0}$ such that

$$\left((\lambda + 2\mu)\frac{\partial u_h^n}{\partial x}, \frac{\partial \phi_h}{\partial x}\right) - \alpha\left(p_h^n, \frac{\partial \phi_h}{\partial x}\right) = \left(f(\cdot, t_n) + \overline{\rho} G \frac{\partial D}{\partial x}, \phi_h\right) + \left[\sigma_N \phi_h\right]\big|_{\Gamma_{MN}}, \tag{11a}$$
$$\forall \phi_h \in V_{h,0},$$

$$(\beta_f \phi p_h^n, \eta_h) + \alpha\left(\frac{\partial u_h^n}{\partial x},\ \eta_h\right) + \tau\left(\frac{\partial {q_f}_h^n}{\partial x}, \eta_h\right) = \frac{\tau}{\rho_f}(g(\cdot, t_n), \eta_h) + (\eta {f}_h^{n-1}, \eta_h), \tag{11b}$$
$$\forall \eta_h \in M_h,$$

$$\left(\left(\frac{\kappa}{\mu_f}\right)^{-1} {q_f}_h^n, \psi_h\right) - \left(p_h^n, \frac{\partial \psi_h}{\partial x}\right) = -\left[p_D(\cdot, t_n)\psi_h n\right]\big|_{\Gamma_{HN}} + \rho_f G\left(\frac{\partial D}{\partial x}, \psi_h\right), \tag{11c}$$
$$\forall \psi_h \in X_{h,0}.$$

Let U^n, P^n, Q_f^n the degrees of freedom of $u_h^n, p_h^n, {q_f}_h^n$ in their bases. Then (11) can be rewritten in the matrix form

$$\begin{bmatrix} A_{uu} & -\alpha A_{pu} & 0 \\ \alpha A_{pu}^T & M_{pp} & \tau A_{q_f p} \\ 0 & -A_{q_f p}^T & M_{q_f q_f} \end{bmatrix} \begin{bmatrix} U^n \\ P^n \\ {Q_f}^n \end{bmatrix} = \begin{bmatrix} \mathscr{F}^n \\ \mathscr{G}^n \\ \mathscr{H}^n \end{bmatrix},\ n \geq 1, \tag{12}$$

where the stiffness and mass matrices $\{A_{uu}, A_{pu}, A_{q_f p}, M_{pp}, M_{q_f q_f}\}$ and vectors $\{\mathscr{F}^n, \mathscr{G}, \mathscr{H}^n\}$ are described in Section 7. The linear system (12) can be further reduced to

$$\mathscr{M}\begin{bmatrix} U^n \\ P^n \end{bmatrix} = \begin{bmatrix} \mathscr{F}^n \\ -\mathscr{G}^n + \tau A_{q_f p} M_{q_f q_f}^{-1} \mathscr{H}^n \end{bmatrix}, \tag{13a}$$

$${Q_f}^n = M_{q_f q_f}^{-1}\left(\mathscr{H}^n + A_{q_f p}^T P^n\right), \tag{13b}$$

where

$$\mathscr{M} = \begin{bmatrix} A_{uu} & -\alpha A_{pu} \\ -\alpha A_{pu}^T & -M_{pp} - \tau A_{q_f p} M_{q_f q_f}^{-1} A_{q_f p}^T \end{bmatrix}. \tag{14}$$

4. Algorithm

The code executes the following steps:

(1) The spatial and temporal grid are generated using the spatial domain end points, $\{a, b\}$, and the final time T_{end} inputted by the user.
   (a) The spatial grid can be uniform or non-uniform. In the first case, the grid size is determined using the number of cells M as an input. For a non-uniform grid, the node positions $\{x_{j+\frac{1}{2}}\}_j$ are inputted.

(b) The temporal grid is uniform, and is generated from the user inputted number of time steps N as $\tau = \dfrac{T_{end}}{N}$.

(2) The physical parameters, boundary conditions, and the initial condition is specified by the user.
(3) The code computes the matrix $\mathscr{M}$ given by (14) and vectors $\{\mathscr{F}^n, \mathscr{G}^n, \mathscr{H}^n\}$ in (13).
(4) At each $n = 1, 2 \ldots, N$, $\{U^n, P^n\}$ are obtained as

$$\begin{bmatrix} U^n \\ P^n \end{bmatrix} = \mathscr{M}^{-1} \begin{bmatrix} \mathscr{F}^n \\ -\mathscr{G}^n + \tau A_{q_f p} M^{-1}_{q_f q_f} \mathscr{H}^n \end{bmatrix}. \tag{15}$$

Then, Q_f^n is obtained from (13b).

4.1. **MATLAB implementation.** The code is run using 4 input parameters:

(1) `el_nodes`: This may be a scalar or a vector. If scalar, then it is the number of cells M and a uniform spatial grid is created with M cells. If it is a vector, then it contains the element nodes $\{x_{j+\frac{1}{2}}\}_{j=0}^{M}$ (nodal grid), starting from $x_{\frac{1}{2}} = a$ and including $x_{M+\frac{1}{2}} = b$.
(2) `ntsteps`: This is an integer that denotes the total number of time steps N. A uniform temporal grid is generated using time step $\tau = \dfrac{T_{end}}{N}$, where $(0, T_{end})$ is the time period of the simulation.
(3) `BC_flags`: This is a 4×1 vector with each entry either 0 or 1. The entry 0 corresponds to Dirichlet boundary condition and 1 corresponds to Neumann boundary condition. The order is determined as [MMHH], i.e., the first two entries correspond to mechanical deformation at $x = a$ and $x = b$, and the last two entries are for hydrological flow (pressure or flux) at $x = a$ and $x = b$; see Section 2.1.
(4) `example`: This is an integer between 1 and 6 which toggles between particular inbuilt examples or a custom scenario: `example` $= 1, 2, 3, 4$ or 5 corresponds to the hard-coded examples demonsrated in Section 5 in this document. `example` $= 6$ corresponds to a custom scenario that needs to be set up by the user.

The code returns the following output:

(1) `xn`: The nodal grid $\{x_{j+\frac{1}{2}}\}_{j=0}^{M}$.
(2) `xcc`: The cell-centered grid $\{x_j\}_{j=1}^{M}$.
(3) `t`: The temporal grid with uniform time step size τ.
(4) `U`: The nodal displacement profile at the final time step.
(5) `P`: The cell-centered pressure profile at the final time step.
(6) `Q`: The nodal flux profile at the final time step.

Example simulation runs:

```
>> [xn, xcc, t, U, P, Q] = Biot1D(10, 10, [0 0 0 0], 1);
>> [xn, xcc, t, U, P, Q] = Biot1D(10, 20, [1 0 0 1], 4);
```

For a complete demonstration of the in-built examples, see Section 5. Additional useful details about some local functions:

(1) The spatial domain and time period may be specified in `grid`.
(2) The physical parmaeters may be changed in `physical_parameters`.
(3) The external sources may be specified in `rhs_f` and `rhs_h`.

Parameter	*Value*	*Unit*
λ	1	[MPa]
μ	1	[MPa]
ϕ	1	[−]
β_f	1	[1/MPa]
κ	1	[m^2]
μ_f	1	[MPa hr]
ρ_f	1.296×10^{13}	[kg/m^3]
G	0	[m/hr^2]

TABLE 2. Parameters used in Example 5.1, Example 5.2, and Example 5.3.

(4) The boundary condition values may be specified by appropriately changing `exact_u`, `exact_du`, `exact_p`, and `exact_qf`.

5. Numerical Examples

In our simulations and examples, we stick to the units of [m] for length, [hr] for time, and [MPa] for pressure.

5.1. **Manufactured solution.**

Example 5.1. *Consider* $\Omega = (0,1)$[m]

$$u(x,t) = -\frac{1}{\pi}\cos(\pi x)\sin\left(\frac{\pi t}{2}\right), \tag{16a}$$

$$p(x,t) = \sin(\pi x)\sin\left(\frac{\pi t}{2}\right),\ \forall x \in (0,1),\ t > 0. \tag{16b}$$

The source terms are

$$f(x,t) = [-(\lambda+2\mu)\pi + \alpha\pi]\cos(\pi x)\sin\left(\frac{\pi t}{2}\right), \tag{17a}$$

$$g(x,t) = \frac{\pi}{2}(\beta_f\phi + \alpha)\sin(\pi x)\cos\left(\frac{\pi t}{2}\right) + \frac{\kappa}{\mu}\pi^2\sin(\pi x)\sin\left(\frac{\pi t}{2}\right). \tag{17b}$$

The physical parameters used in this example are tabulated in Table 2.

The simulation is run over $(0,1)$[hr] using $M = 10$ uniform cells (corresponding to $h = 0.1$[m]), $N = 10$ time steps (corresponding to $\tau = 0.1$[hr]) and all Dirichlet boundary conditions [DDDD] using the following command:

```
>> [xn, xcc, t, U, P, Q] = Biot1D(10, 10, [0 0 0 0], 1);
```

The displacement and pressure profile at the final time step is shown in Figure 1.

Example 5.2. *Consider* $\Omega = (0,1)$[m] *with*

$$u(x,t) = \sin\left(\frac{\pi x}{2}\right)e^{-t}, \tag{18a}$$

$$p(x,t) = \cos\left(\frac{\pi x}{2}\right)e^{-t},\ \forall x \in (0,1),\ t > 0. \tag{18b}$$

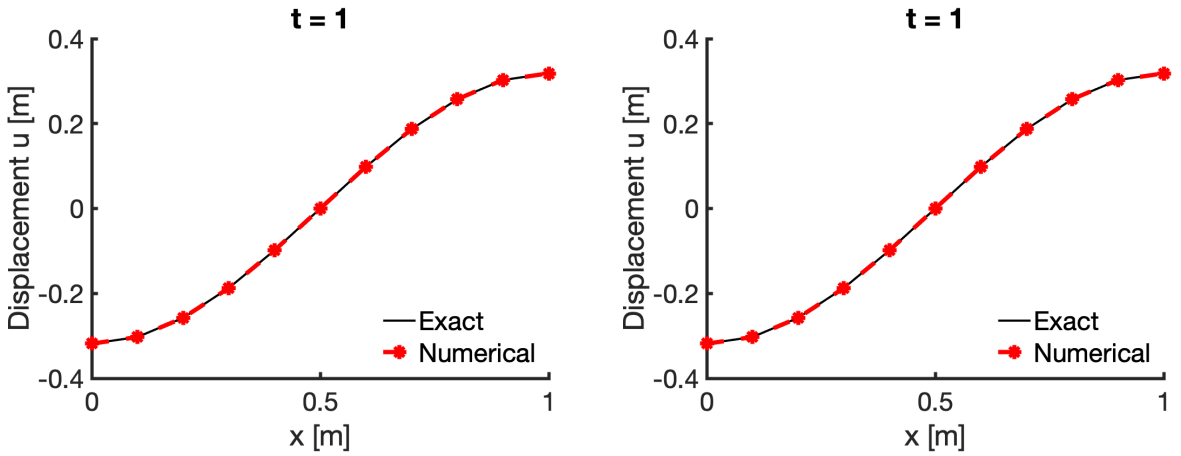

FIGURE 1. Example 5.1: Displacement and pressure profile at the final time step.

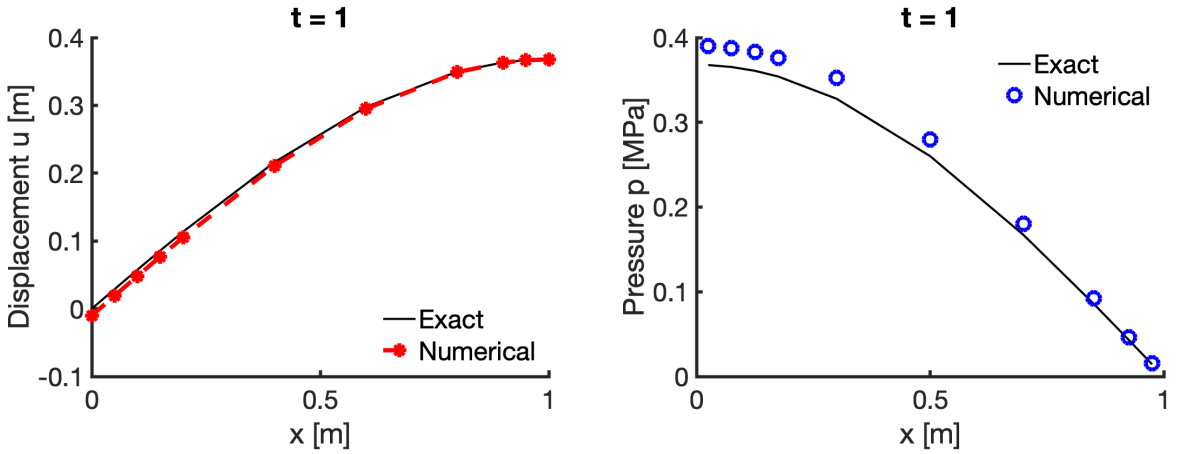

FIGURE 2. Example 5.2: Displacement and pressure profile at the final time step.

The source terms are

$$f(x,t) = \left[(\lambda+2\mu)\frac{\pi^2}{4} - \alpha\frac{\pi}{2}\right]\sin\left(\frac{\pi x}{2}\right)e^{-t}, \tag{19a}$$

$$g(x,t) = \left[-\beta_f\phi - \alpha\frac{\pi}{2} + \frac{\kappa}{\mu_f}\frac{\pi^2}{4}\right]\cos\left(\frac{\pi x}{2}\right)e^{-t}. \tag{19b}$$

The physical parameters used in this example are tabulated in Table 2.

The simulation is run over $(0,1)$[hr] using a non-uniform grid with $M = 10$ cells, $N = 10$ time steps (corresponding to $\tau = 0.1$[hr]), and mixed boundary conditions [NDND] using the following commands:

```
>> el_nodes = [0; 0.05; 0.1; 0.15; 0.2; 0.4; 0.6; 0.8; 0.9; 0.95; 1.0];
>> [xn, xcc, t, U, P, Q] = Biot1D(el_nodes, 10, [1 0 1 0], 2);
```

The displacement and pressure profile at the final time step is shown in Figure 2.

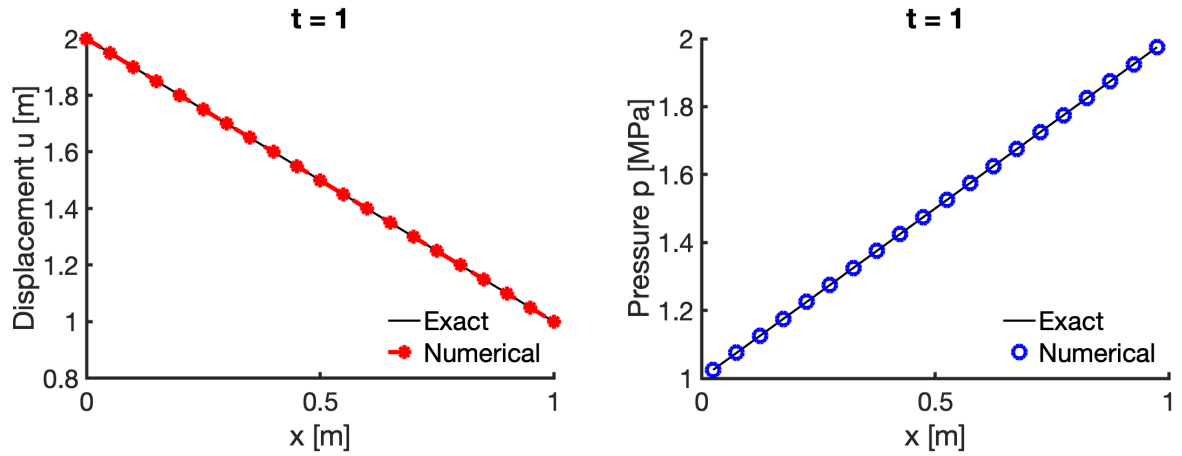

FIGURE 3. Example 5.3: Displacement and pressure profile at the final time step.

Example 5.3. *Consider* $\Omega = (0,1)$[m] *with*

$$u(x,t) = 2 - x, \tag{20a}$$
$$p(x,t) = 1 + x, \ \forall x \in (0,1), \ t > 0. \tag{20b}$$

The source terms are

$$f(x,t) = \alpha, \tag{21a}$$
$$g(x,t) = 0. \tag{21b}$$

The physical parameters used in this example are tabulated in Table 2.

The simulation is run over $(0,1)$[hr] using a uniform grid with $M = 20$ cells (corresponding to $h = 0.05$[m]), $N = 10$ time steps (corresponding to $\tau = 0.1$[hr]), and mixed boundary conditions [DNNN] using the following commands:

```
>> [xn, xcc, t, U, P, Q] = Biot1D(20, 10, [0 1 1 1], 3);
```

The displacement and pressure profile at the final time step is shown in Figure 3.

5.2. **Physical examples.**

Example 5.4. Consolidation test for clay*: This example is inspired from the standard consolidation tests performed at the laboratory scale [4] (Pg. 185). Consider* $\Omega = (0, 0.1)$[m], *with* $x = 0$[m] *being the top of the soil column. The source terms are*

$$f(x,t) = 0, \tag{22a}$$
$$g(x,t) = 0. \tag{22b}$$

We consider the mixed boundary conditions

$$\tilde{\sigma} n = 10^{-1}, \ x = 0, \tag{23a}$$
$$u = 0, \ x = 0.1, \tag{23b}$$
$$p = 0, \ x = 0, \tag{23c}$$
$$q_f = 0, \ x = 0.1. \tag{23d}$$

Parameter	Value	Units	Reference
E	20	[MPa]	[4](Pg. 406)
ν	0.30	[−]	[4](Pg. 406)
ϕ	0.50	[−]	[2](Pg. 74)
β_f	4.16×10^{-4}	[1/MPa]	[6]
κ	1×10^{-17}	[m^2]	[4](Pg. 373)
μ_f	2.7822×10^{-13}	[MPa hr]	[6]
ρ_f	998.21	[kg/m^3]	[6]
ρ_s	2700	[kg/m^3]	[1](Pg. 22)
G	1.27290528×10^8	[m/hr^2]	[6]

TABLE 3. Physical parameters for clay used in Example 5.4.

The physical parameters used in this example are tabulated in Table 3.

The simulation is run over $(0, 24)$[hr] using a uniform grid with $M = 20$ cells (corresponding to $h = 0.005$[m]), $N = 10$ time steps (corresponding to $\tau = 1.2$[hr]), and mixed boundary conditions [NDDN] using the following commands:

```
>> [xn, xcc, t, U, P, Q] = Biot1D(20, 10, [1 0 0 1], 4);
```

The displacement and pressure profiles at $t = 1.2$, $t = 10.8$ and $t = 24$[hr] is shown in Figure 4. The total settlement $s(t) = u(0, t)$ over the simulation period $t \in (0, 24)$[hr] is also shown.

Comments: Clay is highly impermeable. Hence, the pressure decreases gradually the simulation as the water drains out of the soil. At the end of the simulation, steady state has still not been achieved. The settlement curve is qualitatively similar to [4](Pg. 186, Figure 9.26). Also, the effects of gravity are negligible compared to the applied stress of 10^{-1}[MPa] when computing the total settlement: we re-run the simulation without considering the graviational effects (i.e, with $G = 0$[m/hr^2]) get a settlement of $3.694338092420293 \times 10^{-4}$[m], whereas the settlement at the end of the simulation with gravitational effects is $3.709752755037927 \times 10^{-4}$[m].

Example 5.5. Consolidation test for sand and clay: *This example is to demonstrate the robustness of the solver in the presence of heterogeneity. Consider* $\Omega = (0, 1)$[m]*, with* $x = 0$[m] *being the top of the soil column. The source terms are*

$$f(x, t) = 0, \tag{24a}$$
$$g(x, t) = 0. \tag{24b}$$

We consider the mixed boundary conditions

$$\tilde{\sigma} n = 10^{-1}, \ x = 0, \tag{25a}$$
$$u = 0, \ x = 1, \tag{25b}$$
$$p = 0, \ x = 0, \tag{25c}$$
$$q_f = 0, \ x = 1. \tag{25d}$$

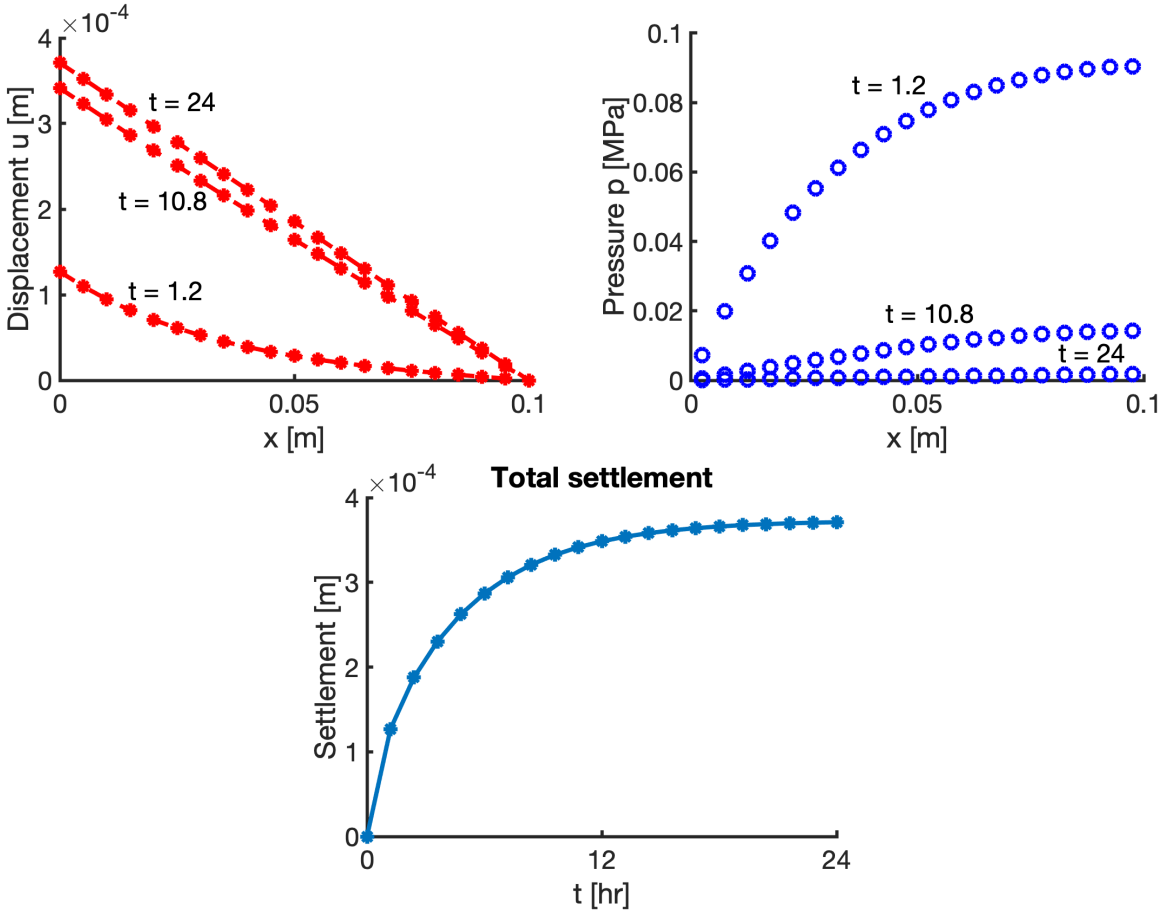

FIGURE 4. Example 5.4: Top row: Displacement and pressure profile at $t = 1.2$, $t = 10.8$ and $t = 24$[hr]. Bottom row: Total settlement over the simulation time period.

We also include the effects of gravity. To introduce heterogeneity, we consider $\Omega = \Omega_{clay} \cup \Omega_{sand}$*, where* $\Omega_{clay} = (0, 0.5)$[m] *and* $\Omega_{sand} = (0.5, 1)$[m]*. We label this case as "Clay over sand". We also consider the case when* $\Omega = \Omega_{sand} \cup \Omega_{clay}$ *with* $\Omega_{sand} = (0, 0.5)$[m] *and* $\Omega_{clay} = (0.5, 1)$[m]*, and we label this case as "Sand over clay". The physical parameters used in this example are tabulated in Table 4.*

The simulation is run over $(0, 8760)$[hr] (i.e., 1[year]) using a uniform grid with $M = 20$ cells (corresponding to $h = 0.05$[m]), $N = 100$ time steps (corresponding to $\tau = 87.6$[hr]), and mixed boundary conditions [NDDN] using the following commands:

```
>> [xn, xcc, t, U, P, Q] = Biot1D(20, 100, [1 0 0 1], 5);
```

The displacement and pressure profiles at the end of the simulation are shown in Figure 4. The total settlement $s(t) = u(0, t)$ over the simulation period $t \in (0, 24)$[hr] is also shown for the two cases.

Comments: Since sand is more permeable than clay, it quickly drains out when it is over clay and the maximum settlement is reached at an early stage compared to the case of clay

Parameter	Value	Units	Reference
E	Clay: 20	[MPa]	[4](Pg. 406)
	Sand: 15	[MPa]	[4](Pg. 407)
ν	Clay: 0.30	[−]	[4](Pg. 406)
	Sand: 0.25	[−]	[4](Pg. 407)
ϕ	Clay: 0.50	[−]	[2](Pg. 74)
	Sand: 0.30	[−]	[2](Pg. 74)
β_f	4.16×10^{-4}	[1/MPa]	[6]
κ	Clay: 1×10^{-17}	[m^2]	[4](Pg. 373)
	Sand: 1×10^{-12}	[m^2]	[4](Pg. 373)
μ_f	2.7822×10^{-13}	[MPa hr]	[6]
ρ_f	998.21	[kg/m^3]	[6]
ρ_s	Clay: 2700	[kg/m^3]	[1](Pg. 22)
	Sand: 2650	[kg/m^3]	[1](Pg. 22)
G	1.27290528×10^8	[m/hr^2]	[6]

TABLE 4. Physical parameters for clay and sand used in Example 5.5.

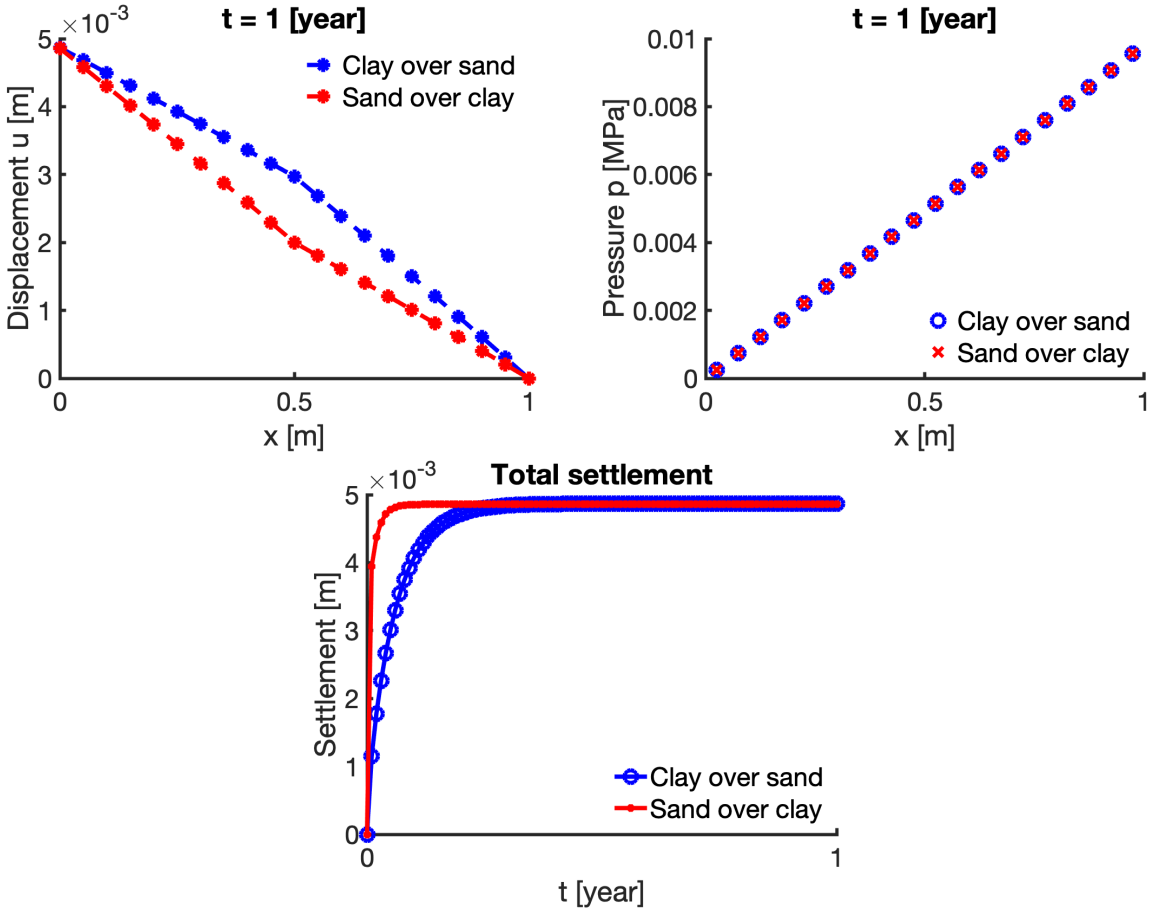

FIGURE 5. Example 5.5: Top row: Displacement and pressure profile at $t = 1$[year]. Bottom row: Total settlement over the simulation time period.

over sand. This is reflected by the settlement curve in Figure 5. The settlement curve is qualitatively similar to [4](Pg. 186, Figure 9.26).

The settlement in the two cases is roughly the same at the end of the simulation: for "Clay over sand" the final settlement is $4.868660654353 \times 10^{-3}$[m] and for "Sand over clay" is $4.858040045928 \times 10^{-3}$.

6. Acknowledgement

This research was partially supported by NSF DMS-1912938 "Modeling with Constraints and Phase Transitions in Porous Media" and NSF DMS-1522734 "Phase transitions in porous media across multiple scales"; PI: Dr. Malgorzata Peszynska.

7. Appendix

Here we give the details of the matrices and vectors computed in Section 3.

7.1. **Approximation spaces bases functions.** We define the basis functions $\{\phi_{j+\frac{1}{2}}\}_{j=0}^{M}$, $\{\eta_j\}_{j=1}^{M}$, and $\{\psi_{j+\frac{1}{2}}\}_{j=0}^{M}$ for $V_h,\ M_h$, and X_h, respectively, defined in 3.1 as follows: $\forall x \in \Omega$

$$\phi_{j+\frac{1}{2}}(x) = \begin{cases} \frac{1}{h_j}\left(x - x_{j-\frac{1}{2}}\right); & x \in \omega_j \\ \frac{1}{h_{j+1}}\left(x_{j+\frac{3}{2}} - x\right); & x \in \omega_{j+1} \\ 0; & \text{otherwise} \end{cases}, \ \forall\ 1 \le j \le M-1, \tag{26}$$

$$\phi_{\frac{1}{2}}(x) = \begin{cases} \frac{1}{h_1}\left(x_{\frac{3}{2}} - x\right); & x \in \omega_1 \\ 0; & \text{otherwise} \end{cases},$$

$$\phi_{M+\frac{1}{2}}(x) = \begin{cases} \frac{1}{h_M}\left(x - x_{M-\frac{1}{2}}\right); & x \in \omega_M \\ 0; & \text{otherwise} \end{cases},$$

$$\eta_j(x) = \begin{cases} 1; & x \in \omega_j \\ 0; & \text{otherwise} \end{cases}, \ \forall\ 1 \le j \le M, \tag{27}$$

$$\psi_{j+\frac{1}{2}} = \phi_{j+\frac{1}{2}}, \ \forall\ 0 \le j \le M, \tag{28}$$

where (28) holds since $H_{div}(I) = H^1(I),\ \forall I \subset \mathbb{R}$.

7.2. **Implementation example using mixed boundary conditions [ND;DN].** Consider (1) with the following mixed boundary conditions

$$\tilde{\sigma} n = \sigma_N,\ x = a, \tag{29a}$$

$$u = u_D,\ x = b, \tag{29b}$$

$$p = p_D,\ x = a, \tag{29c}$$

$$q_f n = q_N,\ x = b. \tag{29d}$$

We denote by $U_j^n = u_h^n(x_{j-\frac{1}{2}}, t_n)$, $P_j^n = p_h^n(x_j, t_n)$, and ${Q_f}_j^n = {q_f}_h^n(x_{j-\frac{1}{2}}, t_n)$. Then we can rewrite

$$u_h^n = \sum_{j=1}^{M} U_j^n \phi_{j-\frac{1}{2}} + u_D(b, t_n)\phi_{M+\frac{1}{2}}, \tag{30a}$$

$$p_h^n = \sum_{j=1}^{M} P_j^n \eta_j, \tag{30b}$$

$$q_{f_h}^n = \sum_{j=1}^{M} {Q_f}_j^n \psi_{j-\frac{1}{2}} + q_N(b, t_n)\psi_{M+\frac{1}{2}}, \tag{30c}$$

Further denote by ${\sigma_N}_{\frac{1}{2}}^n = \sigma_N(a, t_n)$, and ${p_D}_{\frac{1}{2}}^n = p_D(a, t_n)$. The discrete system (11) can be rewritten as

$$\begin{bmatrix} A_{uu} & -\alpha A_{pu} & 0 \\ \alpha A_{pu}^T & M_{pp} & \tau A_{q_f p} \\ 0 & -A_{q_f p}^T & M_{q_f q_f} \end{bmatrix} \begin{bmatrix} U^n \\ P^n \\ {Q_f}^n \end{bmatrix} = \begin{bmatrix} \mathscr{F}^n \\ \mathscr{G}^n \\ \mathscr{H}^n \end{bmatrix}, \ n \geq 1, \tag{31}$$

where the stiffness and mass matrices are

$$A_{uu} = \left[\left((\lambda + 2\mu) \frac{d\phi_{j-\frac{1}{2}}}{dx}, \frac{d\phi_{i-\frac{1}{2}}}{dx} \right) \right]_{1 \leq i,j \leq M}, \tag{32a}$$

$$A_{pu} = \left[\left(\eta_j, \frac{d\phi_{i-\frac{1}{2}}}{dx} \right) \right]_{1 \leq i,j \leq M}, \tag{32b}$$

$$M_{pp} = [(\eta_j, \eta_i)]_{1 \leq i,j \leq M}, \tag{32c}$$

$$A_{q_f p} = \left[\left(\frac{d\psi_{j-\frac{1}{2}}}{dx}, \eta_i \right) \right]_{1 \leq i,j \leq M}, \tag{32d}$$

$$M_{q_f q_f} = \left[\left(\left(\frac{\kappa}{\mu_f} \right)^{-1} \psi_{j-\frac{1}{2}}, \psi_{i-\frac{1}{2}} \right)_T \right]_{1 \leq i,j \leq M}. \tag{32e}$$

The subscript T in (32e) is used to denote the use of the trapezoidal rule to evaluate the integral. This reduces $M_{q_f q_f}$ to a diagonal matrix instead of a tri-diagonal system if full integration were used.

The terms on the right hand side in (31), $\mathscr{F}^n, \mathscr{G}^n$, and $\mathscr{H}^n \in \mathbb{R}^M$ are given by $\forall 1 \leq i \leq M,\ n \geq 1$,

$$\begin{aligned}
\mathscr{F}_i^n &= \left(\left(f(\cdot, t_n) + \overline{\rho} G \frac{\partial D}{\partial x} \right), \phi_{i-\frac{1}{2}} \right) \\
&+ \begin{cases} \sigma_N(a, t_n) & i = 1 \\ 0; & 1 < i < M \\ (\lambda(x_M) + 2\mu(x_M)) \frac{u_D(b,t_n)}{h_M}; & i = M \end{cases}, \qquad (33a) \\
\mathscr{G}_i^n &= h_i \eta_{f_i}^{n-1} \eta_i - \begin{cases} 0; & 1 < i \leq M \\ \alpha u_D(b, t_n) + \tau q_N(b, t_n); & i = M \end{cases}, \qquad (33b) \\
\mathscr{H}_i^n &= \left(\rho_f G \frac{\partial D}{\partial x}, \psi_{i-\frac{1}{2}} \right) + \begin{cases} p_D(a, t_n); & i = 1 \\ 0; & 1 < i \leq M \end{cases}, \qquad (33c)
\end{aligned}$$

where $\forall n \geq 1$,

$$\eta_{f_i}^n = \beta_f \phi(x_i) p_h^n(x_i) + \alpha \frac{\partial u_h^n}{\partial x}(x_i) = \begin{cases} \beta_f \phi(x_i) P_i^n + \alpha \frac{U_{i+\frac{1}{2}}^n - U_{i-\frac{1}{2}}^n}{h_j}; & 1 \leq i < M \\ \beta_f \phi(x_i) P_i^n + \alpha \frac{u_D(b,t_n) - U_{i-\frac{1}{2}}^n}{h_j}; & i = M \end{cases}. \qquad (34)$$

Note: In (33b), for $n = 1$, $\eta_{f_i}^0 = \eta_{f_{init}}(x_i)$ is calculated using the given initial condition (7).

References

[1] Orlando B. Andersland and Branko Ladanyi. *Frozen Ground Engineering*. 2nd ed. Hoboken, NJ : [Reston, Va.]: Wiley; ASCE, 2004. ISBN: 0471615498.

[2] Jacob Bear and Alexander Cheng. *Modeling Groundwater Flow and Contaminant Transport*. Vol. 23. Jan. 2010. ISBN: 978-1-4020-6681-8. DOI: 10.1007/978-1-4020-6682-5.

[3] Maurice A. Biot. "General Theory of Three-Dimensional Consolidation". In: *Journal of Applied Physics* 12.2 (1941), pp. 155–164. DOI: 10.1063/1.1712886.

[4] Jean-Louis Briaud. *Geotechnical Engineering: Unsaturated and Saturated Soils*. Wiley, 2013. ISBN: 9780470948569.

[5] Olivier Coussy. *Poromechanics*. 2004. ISBN: 0-470-84920-7. DOI: 10.1002/0470092718.

[6] *Engineering Toolbox*. https://www.engineeringtoolbox.com. retrieved in 2022.

[7] Phillip Phillips and Mary Wheeler. "A coupling of mixed and continuous Galerkin finite element methods for poroelasticity I: The continuous-in-time case". In: *Computational Geosciences* 11 (June 2007), pp. 145–158. DOI: 10.1007/s10596-007-9044-z.